

High-sensitivity spectroscopic measurements under pulsed high magnetic field

Zheng Wang(王政), Yichun Pan(潘议淳), Guangran Yang(杨光冉), Wei Xie(谢微), and Weihang Zhou(周伟航)
Citation: Chin. Phys. B, 2025, 34 (**7**): 070701. DOI: 10.1088/1674-1056/adce95
http://cpb.iphy.ac.cn; http://iopscience.iop.org/cpb

What follows is a list of articles you may be interested in

Elastic properties of Cu-6wt% Ag alloy wires for pulsed magnets investigated by ultrasonic techniques

Ziyu Li(李滋雨), Tianyi Gu(顾天逸), Wenqi Wei(魏文琦), Yang Yuan(袁洋), Zhuo Wang(王卓), Kangjian Luo(罗康健), Yupeng Pan(潘宇鹏), Jianfeng Xie(谢剑峰), Shaozhe Zhang(张绍哲), Tao Peng(彭涛), Lin Liu(柳林), Qi Chen(谌祺), Xiaotao Han(韩小涛), Yongkang Luo(罗永康), and Liang Li(李亮)
Chin. Phys. B, 2025, 34 (**2**): 020701. DOI: 10.1088/1674-1056/ada1c8

Vector magnetometry in zero bias magnetic field using nitrogen-vacancy ensembles

Chunxing Li(李春兴), Fa-Zhan Shi(石发展), Jingwei Zhou(周经纬), and Peng-Fei Wang(王鹏飞)
Chin. Phys. B, 2024, 33 (**10**): 100701. DOI: 10.1088/1674-1056/ad73af

High-precision nuclear magnetic resonance probe suitable for *in situ* studies of high-temperature metallic melts

Ao Li(李傲), Wei Xu(许巍), Xiao Chen(陈霄), Bing-Nan Yao(姚冰楠), Jun-Tao Huo(霍军涛), Jun-Qiang Wang(王军强), and Run-Wei Li(李润伟)
Chin. Phys. B, 2022, 31 (**4**): 040706. DOI: 10.1088/1674-1056/ac4a70

Spectroscopic measurements and terahertz imaging of the cornea using a rapid scanning terahertz time domain spectrometer

Wen-Quan Liu(刘文权), Yuan-Fu Lu(鲁远甫), Guo-Hua Jiao(焦国华), Xian-Feng Chen(陈险峰), Zhi-Sheng Zhou(周志盛), Rong-Bin She(佘荣斌), Jin-Ying Li(李金瑛), Si-Hai Chen(陈四海), Yu-Ming Dong (董玉明), Jian-Cheng Lü(吕建成)
Chin. Phys. B, 2016, 25 (**6**): 060702. DOI: 10.1088/1674-1056/25/6/060702

INSTRUMENTATION AND MEASUREMENT

High-sensitivity spectroscopic measurements under pulsed high magnetic field

Zheng Wang(王政)[1], Yichun Pan(潘议淳)[1], Guangran Yang(杨光冉)[1], Wei Xie(谢微)[2], and Weihang Zhou(周伟航)[1,†]

[1] *Wuhan National High Magnetic Field Center and School of Physics, Huazhong University of Science and Technology, Wuhan* 430074, *China*
[2] *State Key Laboratory of Precision Spectroscopy, School of Physics and Electronic Science, East China Normal University, Shanghai* 200241, *China*

(Received 20 January 2025; revised manuscript received 9 April 2025; accepted manuscript online 21 April 2025)

Pulsed magnet technology is the only way to generate ultra-strong magnetic fields higher than 45 T so far. However, the inherently fast-changing field strength (typically on the order of 1000 T/s) poses significant challenges for spectroscopic measurements which rely on time integration of signals to improve spectral qualities. In this work, we report high-sensitivity spectroscopic measurements under pulsed high magnetic fields employing the long flat-top pulsed magnetic field technique. By means of a multiple-capacitor power supply, we were able to generate pulsed high magnetic fields with controllable flat-top pulse width and field stabilities. By synchronizing spectroscopic measurements with the waveform of the flat-top magnetic field, the integration time of each spectrum can be increased by up to 100 times compared with that of the conventional spectroscopic measurements under pulsed magnetic fields, thus enabling high-sensitivity spectroscopic measurements under ultra-strong pulsed magnetic fields. These findings promise an efficient way to significantly improve the performance and extend the application of optical measurements under pulsed high magnetic fields.

Keywords: pulsed magnet, flat-top pulsed magnetic field, optical spectroscopy, photoluminescence

PACS: 07.57.Pt, 07.55.–w, 07.55.Db

DOI: 10.1088/1674-1056/adce95 **CSTR:** 32038.14.CPB.adce95

1. Introduction

High magnetic field has pronounced effects on magnetic moments of materials. It is capable of altering electron spin and orbital states, thereby engineering the properties of materials. Thanks to the rapid progresses in the past decades, high magnetic field has become an important extreme experimental condition that has significant applications in cutting-edge scientific research across various disciplines, such as physics, chemistry, materials science and biomedicine. On the other hand, with the advantages of non-contact operation, high precision and fast analysis speed, spectral measurements represent one of the most powerful tools for characterization of materials. The combination of high magnetic field with spectral measurement techniques, i.e., magneto-spectroscopy, will undoubtedly play a key role in promoting scientific research in materials science. Indeed, the successful application of magneto-spectroscopy has led to plenty of significant breakthroughs at the forefront of condensed matter physics. By means of absorption spectroscopy measurements in high magnetic field, Miyata *et al.*[1] measured precisely the exciton binding energy and effective masses for charge carriers in organic-inorganic tri-halide perovskites, providing crucial information about the photophysics of these materials. In a similar way, Goryca *et al.*[2] successfully revealed a series of essential material parameters for monolayer transition metal dichalcogenide semiconductors. With the help of high magnetic field spectroscopy, quantum correlation among charge carriers, which leads to the generation of superfluorescence/superradiance, can be elucidated, as reported by Timothy *et al.*[3] for plasma in semiconductor quantum wells. Additionally, much intriguing physics, such as brightening of dark excitons,[4–6] quantum chaos of shallow impurities in semiconductors[7,8] and the Aharonov–Bohm effect,[9–11] has also been revealed through magneto-spectroscopy.

Considering the significant role of high magnetic field, technologies capable of generating high magnetic field have become the focus of attention over the past few decades. Due to the severe challenges brought by Joule heating and electromagnetic forces, pulsed magnet technology has become the only way to generate ultra-strong magnetic fields higher than 45 T so far. Thanks to the advancement in magnet technology, non-destructive pulsed magnets are now capable of generating strong magnetic fields as high as 100 T. There's no doubt that such pulsed high magnetic fields have made significant contributions to the rapid development of both fundamental science and industrial applications.[12–17] However, as intrinsic characteristics of pulsed magnets, the fast-changing field strength (typically on the order of 1000 T/s) poses severe chal-

†Corresponding author. E-mail: zhouweihang@hust.edu.cn

© 2025 Chinese Physical Society and IOP Publishing Ltd. All rights, including for text and data mining, AI training, and similar technologies, are reserved.

lenges for spectroscopic measurements as they rely on time integration of signals to improve spectral qualities. For this reason, spectroscopic measurements under pulsed high magnetic fields have long been limited to samples with strong emission/absorption signals. Lots of novel materials and structures with weak optical signals but significant applications cannot be studied spectroscopically under pulsed high magnetic fields. Therefore, the development of new spectroscopic measurement techniques with high detection sensitivity under pulsed strong magnetic fields has long been a pursued goal in scientific communities.[18]

In this work, we report the development of a high-sensitivity spectroscopic measurement technique under pulsed high magnetic field. This new technique was developed on the basis of long flat-top pulsed magnetic fields[19–23] — a magnetic field generation technology which possesses both the high field strength characteristic of pulsed magnets and the advantage of high stability inherent in steady-state magnets. Through the introduction of a multiple-capacitor power supply, we were able to generate pulsed magnetic fields with maximum field strength of 50 T and pulse width of flat-top up to 100 ms. By means of precise synchronization among the pulsed field, external light source and the spectral detector, the integration time of a single spectrum was successfully increased up to 100 times compared with that of the conventional spectroscopic measurement schemes in pulsed magnetic field. High-sensitivity spectroscopic measurements are thus made possible under pulsed ultra-high magnetic fields.

2. System overview

A schematic diagram of our spectroscopic measurement system under pulsed high magnetic field is shown in Fig. 1. The system is primarily composed of four sub-systems, including external light sources, a spectrometer, a delay/pulse generator and a pulsed magnet. The pumping beam from external light sources is guided onto samples placed in the center of the bore of the pulsed magnet through optical fibers. The emitted/reflected signal is guided out of the magnet using another optical fiber with a relatively larger core diameter and transferred to a spectrometer, where the signal is spectrally analyzed and detected. As pointed out in the previous text, the magnetic field generated by a pulsed magnet system changes very fast with time and typically lasts only tens to hundreds of milliseconds. Therefore, synchronization among the magnet, the detector and light sources is very important. To do this, we use a delay/pulse generator to control precisely the trigger time of these devices. To avoid unwanted heating of the samples by the pumping beam, a high-speed optical shutter is incorporated into the optical path to control the excitation time of the samples. The magnetic field generated by the pulsed magnet is detected by a home-built pickup coil which operates based on Faraday's law of electromagnetic induction. The induction signal from the pickup coil, as well as the feedback transistor-transistor logic (TTL) signals from the optical shutter and charge-coupled device (CCD) detector, is recorded by a data acquisition card and subsequently processed by a computer.

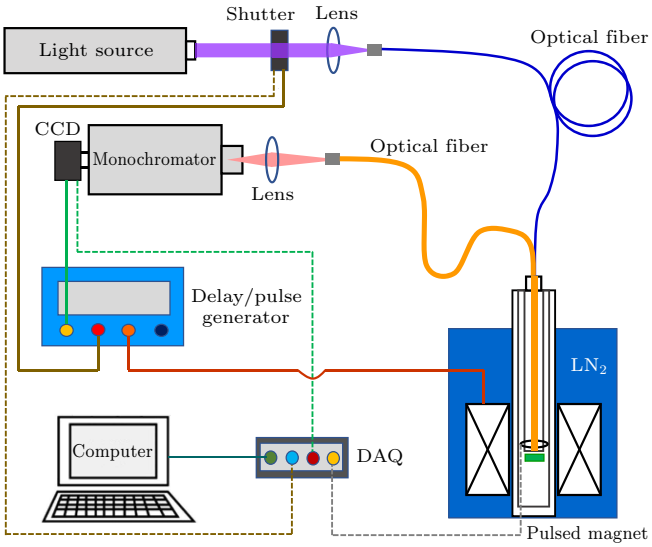


Fig. 1. Schematic diagram of spectroscopic measurement system under pulsed high magnetic field. DAQ: data acquisition card. CCD: charge-coupled device. LN_2: liquid nitrogen.

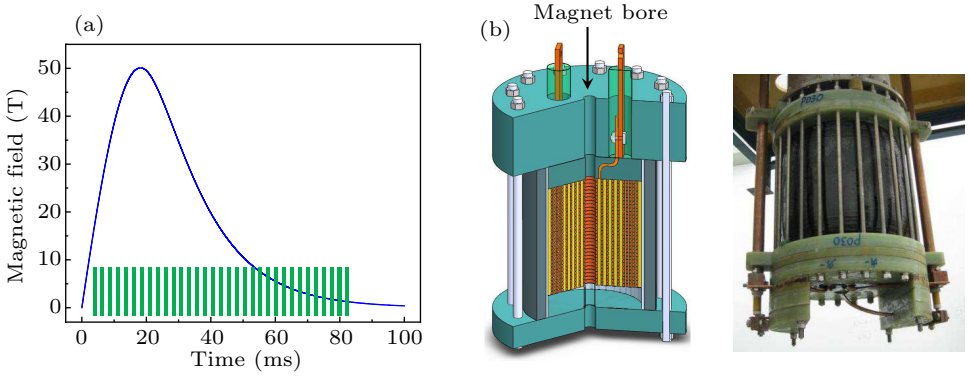


Fig. 2. (a) Typical waveform of magnetic field generated by a pulsed magnet. The vertical green lines represent trigger signals for spectral measurements. (b) Left: schematic diagram showing the internal structure of a pulsed magnet. Right: a photo of a real pulsed magnet from Wuhan National High Magnetic Field Center.

For comparison, Fig. 2(a) shows the typical waveform of magnetic fields generated by a pulsed magnet. As one can see, the magnetic field increases from 0 to 50 T in just $\sim$ 15 ms and then drops to zero again in less than 80 ms, demonstrating its inherent characteristics of fast-changing field strength. To address this challenge, the integration time of a single spectrum is usually reduced to $\sim$ 1 ms in conventional spectroscopic measurements in pulsed magnetic fields. High-speed detectors, such as electron multiplying charge-coupled device (EMCCD) and intensified charge-coupled device (ICCD), are typically introduced to record consecutively a series of spectra in a single pulse of magnetic field, as illustrated schematically by the vertical green lines in Fig. 2(a). A schematic diagram as well as a photo of the pulsed magnet is given in Fig. 2(b), for the readers' convenience.

3. Design of optical probe

In sharp contrast to commercial superconducting magnets, the bore of pulsed magnets is usually very small (typically around 10 mm) and filled with liquid nitrogen as the whole magnet is immersed into liquid nitrogen to deal with Joule heating. Moreover, severe mechanical vibration is inevitable for pulsed magnets due to the huge pulsed current injected by the power system. Considering these limiting conditions, optical fibers are the most appropriate choice to make optical probes for spectroscopic measurements under pulsed high magnetic field. We designed four sets of optical probes for different types of measurements. The optical probe for photoluminescence measurements is shown schematically in Fig. 3(a). A fiber bundle is used to guide the pumping laser (photoluminescence signal) into (out of) the pulsed magnet. Here, the central fiber with larger core diameter is used to guide the laser beam. The outer array of fibers with smaller core diameter is used to collect signals emitter by samples. An optional thin-film polarizer can be inserted between the fiber bundle and samples for polarization-resolved photoluminescence measurements. The setup of optical probe for reflectivity measurements is plotted in Fig. 3(b). It has a very similar structure to the optical probe for photoluminescence measurements, except that the fiber bundle is replaced by a multi-mode fiber. In contrast, optical probes for absorption (transmission) measurements are quite different from those for photoluminescence and reflectivity measurements. The optical probe for transmission measurements under Faraday configuration is shown in Fig. 3(c). We use two optical fibers with different core diameters to guide light beams. The small core fiber is used to guide the incident white light beam to the samples. The relatively larger fiber is used to collect the transmitted light beam as larger fibers can increase the signal collection efficiency. Two small-sized prisms are introduced to construct the complete optical path. Figure 3(d) shows schematically the setup of optical probe for transmission measurements under Voigt configuration. Compared with that for Faraday configuration as shown in Fig. 3(c), the main difference is that the samples and polarizers are sandwiched between the two prisms.

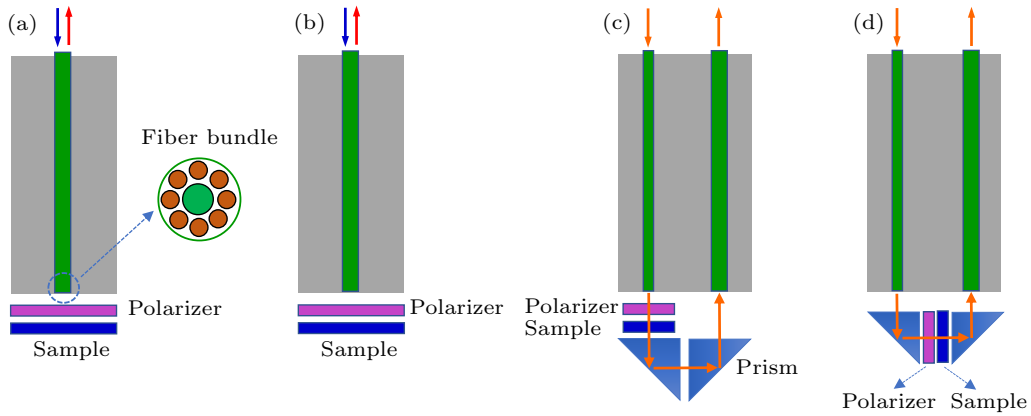


Fig. 3. Design of optical probes with different configurations. (a) Optical probe for photoluminescence measurements. (b) Optical probe for reflectivity measurements. (c) Optical probe for transmission measurements under Faraday configuration. (d) Optical probe for transmission measurements under Voigt configuration. The pulsed magnetic field is applied along the vertical direction.

4. Generation of flat-top pulsed magnetic field

As pointed out in the previous text, the severest challenge for spectroscopic measurements in pulsed high magnetic fields is their rapidly-changing field strength. This inherent characteristic reduces the typical integration time of spectral measurements under pulsed magnetic field to $\sim$ 1 ms, which in turn significantly limits the application of magneto-spectroscopy under pulsed high magnetic fields. To address this challenge, we introduced a special type of pulsed magnetic field — flat-top pulsed magnetic field. For flat-top pulsed magnetic fields, the field strength can remain constant for a period of time after reaching its peak value. Therefore, they possess the advantages of both the high field strength of pulsed magnets and the good stability of steady-state magnets.

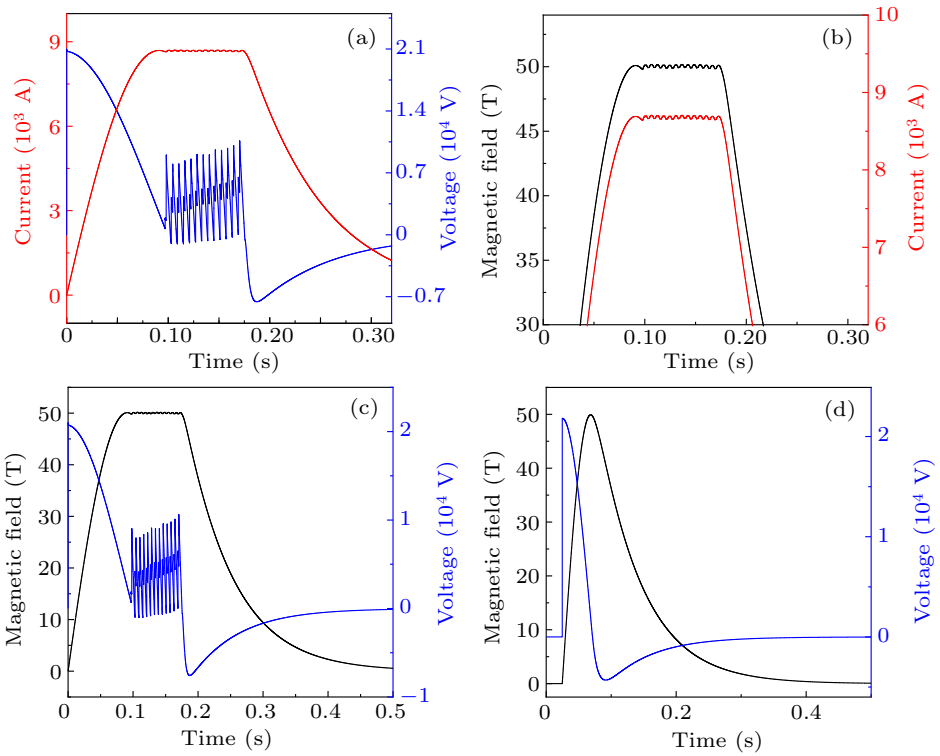


Fig. 4. Generation of flat-top pulsed magnetic fields through multiple-capacitor power supply scheme. (a) Simulated time-dependent current and voltage applied to a pulsed magnet. (b) Simulated current and the resulting magnetic field for a pulsed magnet. (c) Simulated magnetic field and the externally applied voltage. (d) Simulated field strength and the applied voltage for conventional non-flat-top pulsed magnetic field.

In our work, we employed a multiple-capacitor power supply scheme to generate flat-top pulsed high magnetic fields. The pulsed magnet system can be regarded as an resistor–lnductor–capacitor (RLC) circuit. The strength of the magnetic field generated by the solenoid coil is directly proportional to the magnitude of the current passing through it. Therefore, we can control the waveform of the pulsed magnetic field through that of the pulsed current injected into the magnet. In Wuhan National High Magnetic Field Center, the pulsed magnets are powered by a series of independent capacitor banks. Both charging and discharging parameters for these capacitor banks can be controlled independently. The sequential discharge of a series of capacitor banks based on designed time series and voltages can yield a flat-top pulsed magnetic field. We calculate the discharge parameters of multiple capacitor banks through a hybrid algorithm based on the genetic algorithm and particle swarm optimization. The theoretically predicted waveforms for the applied voltage, current and magnetic field, modeled in MATLAB/Simulink, are plotted in Figs. 4(a)–4(c). Figure 4(a) shows the applied voltage and the resulting current as a function of time. Each spike in the voltage curve represents the discharge of an additional capacitor bank. The superposition of these sequential discharging curves leads to a broad current waveform with a flat top, as illustrated by the red curve in Fig. 4(a). As the generated magnetic field is proportional to the current passing through the magnet (Fig. 4(b)), the flat-top current directly yields a flat-top pulsed magnetic field, as shown by the black curve in Fig. 4(c). As both charging and discharging parameters can be controlled flexibly, the magnetic field waveform can be tailored conveniently. As an example, we show the magnetic field generated by the same magnet but different discharging parameters in Fig. 4(d), where a conventional waveform of the magnetic field can be clearly identified. Using our method, both the width and ripple of the flat top of the pulsed magnetic field can be adjusted in real time.

Figure 5 shows the measured flat-top pulsed magnetic fields generated by the multiple-capacitor power supply scheme discussed above. As one can see, the experimental waveforms are in very good agreement with theoretical predictions. The width of the flat top is about 100 ms and the highest field is $\sim$ 50 T (limited by the available capacitor banks).

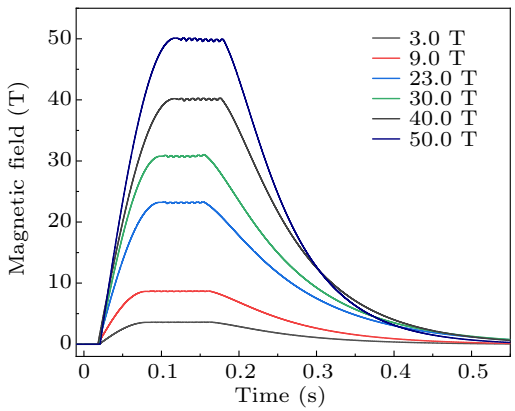


Fig. 5. Typical flat-top pulsed magnetic fields generated by the multiple-capacitor power supply scheme.

5. Spectroscopic measurements

To study directly the effects of pulse width of magnetic field on spectroscopic measurements, we carried out spectral measurements under both conventional and flat-top pulsed magnetic fields. The samples we used are mechanically exfoliated InSe flakes, which are typical two-dimensional layered semiconductors that have received much attention in the past decades. The measured photoluminescence spectra pumped by a 532 nm continuous wave laser at a temperature of 170 K are plotted in Fig. 6. For easy direct comparison, we first measured the samples under pulsed magnetic field with a conventional waveform. In this case, the spectral integration time must be set very short as the field strength changes very fast (Fig. 6(e)). The spectrum obtained with an integration time of 1 ms, which is typically adopted in pulsed magnetic field spectral measurements, is shown in Fig. 6(a). As one can see, no spectral features can be distinguished due to the insufficient exposure time of the CCD detector.

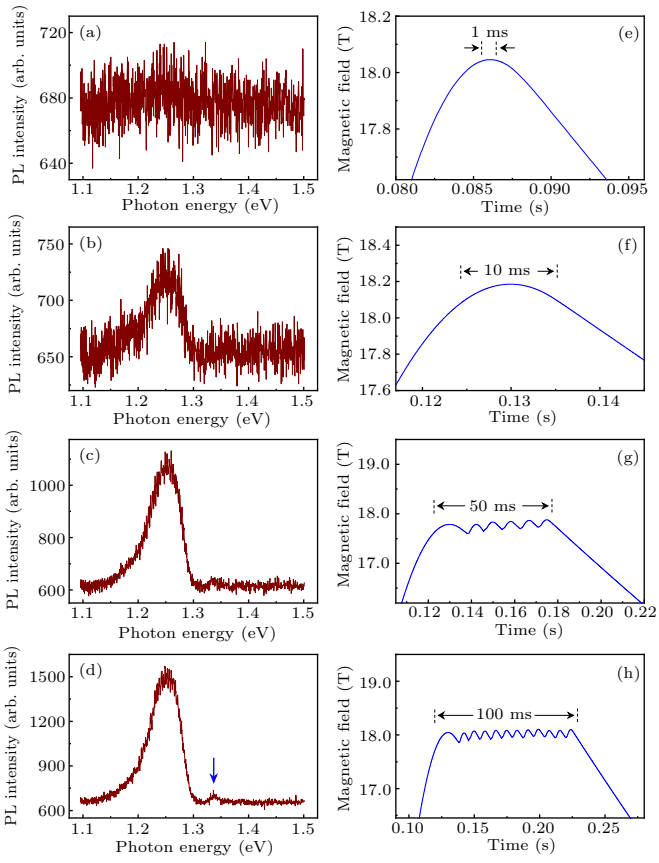


Fig. 6. Photoluminescence spectra of mechanically exfoliated InSe flakes under pulsed high magnetic fields with different pulse widths. Measured photoluminescence spectrum with integration time of (a) 1 ms, (b) 10 ms, (c) 50 ms, and (d) 100 ms. (e) Magnified view of a conventional pulsed magnetic field waveform near its peak region. (f) Magnified view of a pulsed magnetic field with larger pulse width. (g) A flat-top pulsed magnetic field whose flat top width is $\sim$ 50 ms. (h) A flat-top magnetic field whose flat top width is $\sim$ 100 ms. The numbers given in (e)–(h) denote the available integration time for one spectrum. All photoluminescence spectra were taken at 170 K using a 532 nm continuous wave laser.

Figure 6(b) shows the photoluminescence spectrum when the integration time was increased to 10 ms. To do this, we increased the pulse width of the magnetic field through the multiple-capacitor power supply scheme. As illustrated, an emission peak at $\sim$ 1.25 eV,[24,25] which stems from excitons of bulk InSe, can be identified. However, minor spectral structures that probably exist cannot be distinguished due to the poor signal-to-noise ratio. In Fig. 6(g), we generated a flat-top pulsed magnetic field with a flat-top width of $\sim$ 50 ms. In this case, the spectral integration time can be increased to 50 ms as well. The resulting spectrum is plotted in Fig. 6(c). The spectral quality is improved significantly. Using the multiple-capacitor power supply scheme, we eventually increased the width of the flat top up to $\sim$ 100 ms, as shown in Fig. 6(h). The corresponding photoluminescence spectrum is plotted in Fig. 6(d). In addition to the main emission peak, a minor structure at $\sim$ 1.34 eV, [26–28] as highlighted by a blue arrow, can also be identified unambiguously.

To quantify the evolution of the signal-to-noise ratio of the magneto-spectra in flat-top magnetic fields, we calculated the signal-to-noise ratio using the measured spectra. The corresponding results are shown in Fig. 7. Here, the signal-to-noise ratio is defined as $\mathrm{SNR} = I_{\mathrm{signal}}/\sigma_{\mathrm{noise}}$, where I_{signal} represents the peak intensity of the spectrum and σ_{noise} is the standard deviation of noise. As one can see from the figure, the signal-to-noise ratio shows threshold-like behaviors as a function of the flat top width (integration time). Such behaviors demonstrate clearly the importance of flat-top pulsed magnetic fields for spectroscopic measurements, as such long integration time is only possible when flat-top magnetic fields are introduced.

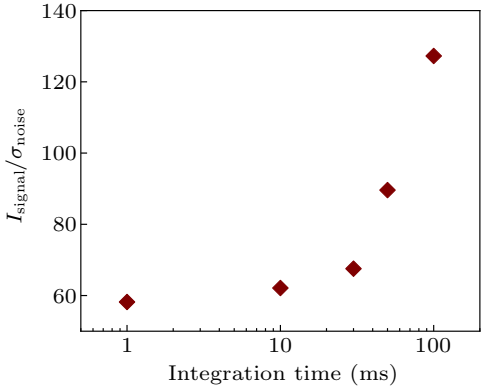


Fig. 7. Signal-to-noise ratio of the magneto-spectra as a function of the width of the flat top.

For the purpose of a straightforward comparison, the photoluminescence spectrum taken under 50 T pulsed magnetic field with a flat top width of 100 ms is plotted together with that taken under zero magnetic field, as shown in Fig. 8. The minor structure at $\sim$ 1.34 eV comes from excitons of thin InSe flakes. As one can see, excitonic emission behaviors of thick

and thin flakes respond differently to external magnetic fields as a result of the quantum confinement effect. While exciton emission from thin flakes is enhanced significantly by the pulsed magnetic field, exciton emission of thick flakes shows only slight enhancement.

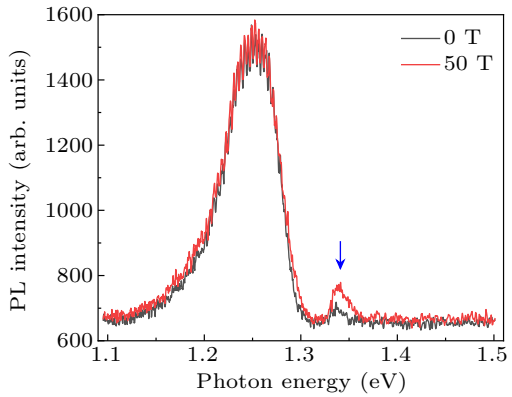


Fig. 8. Effect of high magnetic field on the photoluminescence of exfoliated InSe flakes. Black curve: without magnetic field. Red curve: taken under 50 T magnetic field. Sample temperature: 170 K. Pumping laser: 532 nm continuous wave laser.

6. Conclusion and perspectives

In summary, we report the development of a high-sensitivity spectroscopic measurement technique under pulsed high magnetic fields. Through the introduction of a multiple-capacitor power supply scheme, we were able to generate flat-top pulsed high magnetic fields with a flat top width of $\sim$ 100 ms and maximum field of $\sim$ 50 T. By synchronizing the pulsed magnetic field, the detector and the light source, we successfully increased the spectral integration time to 100 ms, which is up to 100 times longer than that adopted in conventional spectral measurements in pulsed high magnetic fields. High-sensitivity spectral measurements in pulsed magnetic fields are thus made possible. Our technique represents an efficient solution for high signal-to-noise ratio spectral measurements in pulsed high magnetic fields.

Acknowledgements

This work was financially supported by the National Key Research and Development Program of China (Grant No. 2022YFA1602700) and the National Natural Science Foundation of China (Grant No. 12274159).

References

[1] Miyata A, Mitioglu A, Plochocka P, Portugall O, Wang J T W, Stranks S D, Snaith H J and Nicholas R J 2015 *Nat. Phys.* **11** 582
[2] Goryca M, Li J, Stier A V, Taniguchi T, Watanabe K, Courtade E, Shree S, Robert C, Urbaszek B, Marie X and Crooker S A 2019 *Nat. Commun.* **10** 4172
[3] Timothy Noe Ii G, Kim J H, Lee J, Wang Y, Wójcik A K, McGill S A, Reitze D H, Belyanin A A and Kono J 2012 *Nat. Phys.* **8** 219
[4] Zhang X X, Cao T, Lu Z, Lin Y C, Zhang F, Wang Y, Li Z, Hone J C, Robinson J A, Smirnov D, Louie S G and Heinz T F 2017 *Nat. Nanotechnol.* **12** 883
[5] Feierabend M, Brem S, Ekman A and Malic E 2020 *2D Mater.* **8** 015013
[6] Boekhoven J 2018 *Nat. Nanotechnol.* **13** 979
[7] Chen Z, Zhou W, Zhang B, Yu C H, Zhu J, Lu W and Shen S C 2009 *Phys. Rev. Lett.* **102** 244103
[8] Zhou W, Chen Z, Zhang B, Yu C H, Lu W and Shen S C 2010 *Phys. Rev. Lett.* **105** 024101
[9] Overstreet C, Asenbaum P, Curti J, Kim M and Kasevich M A 2022 *Science* **375** 226
[10] Vaidman L 2012 *Phys. Rev. A* **86** 040101
[11] Caprez A, Barwick B and Batelaan H 2007 *Phys. Rev. Lett.* **99** 210401
[12] Portugall O, Puhlmann N, Müller H U, Barczewski M, Stolpe I and Ortenberg M v 1999 *J. Phys. D: Appl. Phys.* **32** 2354
[13] Li L, Ding H, Peng T, Han X, Xia Z, Chen J, Duan X, Wang C, Pan Y, Vanacken J and Herlach F 2008 *IEEE Trans. Appl. Supercond.* **18** 596
[14] Liu S, Peng T, Liu X, Shang H, Wang S, Pan Z, Jin G, Li J and Li L 2024 *IEEE Trans. Appl. Supercond.* **34** 1
[15] Peng T, Liu S B, Pan Y, Lv Y L, Ding H F, Han X T, Xiao H X, Wang S, Jiang S and Li L 2022 *IEEE Trans. Appl. Supercond.* **32** 1
[16] Li Z Y, Gu T Y, Wei W Q, Yuan Y, Wang Z, Luo K J, Pan Y P, Xie J F, Zhang S Z, Peng T, Liu L, Chen Q, Han X T, Luo Y K and Li L 2025 *Chin. Phys. B* **34** 049901
[17] Xie J F, Zhang S Z, Shi J T, Wang J F, Li L and Han X T 2023 *High Voltage.* **8** 898
[18] Tay F, Baydin A, Katsutani F and Kono J 2022 *J. Phys. Soc. Jpn.* **91** 101006
[19] Wei W, Liu Q, Yuan L, Zhang J, Liu S, Zhou R, Luo Y and Han X 2023 *IEEE Trans. Instrum. Meas.* **72** 1
[20] Xu Y, Gao Z, Yan Z, Chen J and Zhao C 2024 *IEEE Trans. Appl. Supercond.* **34** 1
[21] Wang S, Peng T, Jiang F, Jiang S, Chen S, Deng L, Huang R and Li L 2020 *IEEE Trans. Appl. Supercond.* **30** 1
[22] Xiao H, Ma Y, Lv Y, Ding T, Zhang S, Hu F, Li L and Pan Y 2014 *IEEE Trans. Power Electron.* **29** 4532
[23] Kohama Y and Kindo K 2015 *Rev. Sci. Instrum.* **86** 104701
[24] Geng J, Zhang D, Kim I, Kim H M, Higashitarumizu N, Rahman I K M R, Lam L, Ager J W, Davydov A V, Krylyuk S and Javey A 2024 *Adv. Funct. Mater.* **35** 2413672
[25] Nelson J, Stanev T K, Lebedev D, Lamountain T, Gish J T, Zeng H, Shin H, Heinonen O, Watanabe K, Taniguchi T, Hersam M C and Stern N P 2023 *Phys. Rev. B* **107** 115304
[26] Brotons-Gisbert M, Andres-Penares D, Suh J, Hidalgo F, Abargues R, Rodríguez-Cantó P J, Segura A, Cros A, Tobias G, Canadell E, Ordejón P, Wu J, Martínez-Pastor J P and Sánchez-Royo J F 2016 *Nano Lett.* **16** 3221
[27] Li C, Zhao L, Shang Q, Wang R, Bai P, Zhang J, Gao Y, Cao Q, Wei Z and Zhang Q 2022 *ACS Nano* **16** 1477
[28] Debbichi L, Eriksson O and Lebègue S 2015 *J. Phys. Chem. Lett.* **6** 3098